Gain Modulation from Background Synaptic Input

Frances S. Chance,[1,3] L.F. Abbott,[2]
and Alex D. Reyes[1]
[1]Center for Neural Science
New York University
New York, New York 10003
[2]Volen Center for Complex Systems and
Department of Biology
Brandeis University
Waltham, Massachusetts 02454

Summary

Gain modulation is a prominent feature of neuronal activity recorded in behaving animals, but the mechanism by which it occurs is unknown. By introducing a barrage of excitatory and inhibitory synaptic conductances that mimics conditions encountered in vivo into pyramidal neurons in slices of rat somatosensory cortex, we show that the gain of a neuronal response to excitatory drive can be modulated by varying the level of "background" synaptic input. Simultaneously increasing both excitatory and inhibitory background firing rates in a balanced manner results in a divisive gain modulation of the neuronal response without appreciable signal-independent increases in firing rate or spike-train variability. These results suggest that, within active cortical circuits, the overall level of synaptic input to a neuron acts as a gain control signal that modulates responsiveness to excitatory drive.

Introduction

Neurons in vivo are continuously bombarded by synaptic input, which dramatically affects their response properties (Destexhe and Paré, 1999; Hô and Destexhe, 2000; Tiesinga et al., 2001; Anderson et al., 2000a) by increasing overall conductance (Borg-Graham et al., 1998; Hirsch et al., 1998; Destexhe and Paré, 1999) and introducing a high degree of response variability (Softky and Koch, 1993; Holt et al., 1996; Stevens and Zador, 1998; Shadlen and Newsome, 1994; Troyer and Miller, 1997). Typically, this background activity is treated as a constant source of noise that continuously underlies the stimulus-evoked increases in excitation that drive neuronal responses. Here we consider the impact of varying the level of background activity. We find that changing the level of background input, rather than affecting response variability, modulates the gain of neuronal responses. Our results suggest that the gain modulation commonly seen in vivo may arise from varying levels of background synaptic input.

Gain modulation is a primary mechanism by which cortical neurons combine and process information (for a review, see Salinas and Thier, 2000). It appears in a wide range of contexts, including the gaze-direction dependence of visual neurons in posterior parietal cortex (Andersen and Mountcastle, 1983; Andersen et al., 1985), the effects of attention (McAdams and Maunsell, 1999a; Treue and Martínez-Trujillo, 1999), and as a possible basis for a variety of "nonclassical" receptive field effects in primary visual cortex (Heeger, 1992). Gain modulation has also been proposed as a mechanism for the neural computation of coordinate transformations relevant for tasks ranging from visually guided reaching (Zipser and Andersen, 1988; Salinas and Abbott, 1995; Pouget and Sejnowski, 1997) to invariant object recognition (Salinas and Abbott, 1997).

Gain modulation is not equivalent to the enhancement or suppression of neuronal responses by pure excitation or inhibition. To illustrate the distinction, consider the firing rate of a neuron in response to injected current (which we call driving current) shown schematically in Figure 1A. Increased excitation shifts the firing-rate curve to the left, and increased inhibition, whether of the hyperpolarizing or shunting variety (Holt and Koch, 1997), shifts it to the right (as discussed below, see Figure 3A). Gain modulation, on the other hand, is a change in the slope of the firing-rate curve, corresponding to a multiplicative or divisive scaling, which is distinct from these additive or subtractive shifts. Mechanisms that generate true gain modulation from fast, ionotropic synaptic input have proven elusive (Srinivasan and Bernard, 1976; Koch and Poggio, 1992; Mel, 1993; Salinas and Abbott, 1996; Hahnloser et al., 2000; Doiron et al., 2001; Smith et al., 2002).

The background synaptic input we study is primarily in the balanced configuration proposed to exist in cortical circuits (Shadlen and Newsome, 1994; Troyer and Miller, 1997). In this configuration, excitatory and inhibitory components approximately cancel, keeping the average total synaptic current near zero. Although a balanced configuration is not a strict requirement for the results we present, it has the advantage that the level of background activity can be modified independently of excitatory synaptic drive if excitatory and inhibitory inputs are modulated in parallel, specifically if their input rates are scaled by the same factor. Conversely, the overall level of excitatory drive can be modified without changing the total synaptic input to a neuron if excitatory and inhibitory rates are modulated in an opposing or push-pull manner (Anderson et al., 2000b). Thus, the excitatory drive and the total level of synaptic input can be modulated independently and comprise two separate input channels. Traditionally, the push-pull channel has been considered to be the primary information conduit to the neuron. Here, we find that the "noise" channel, consisting of the overall level of synaptic input, can carry a second, independent control signal that modulates the gain of neuronal responses.

Results

Introducing In Vivo Synaptic Input
into In Vitro Neurons
To show how background synaptic input modulates the gain of neuronal responses, we introduced conductance
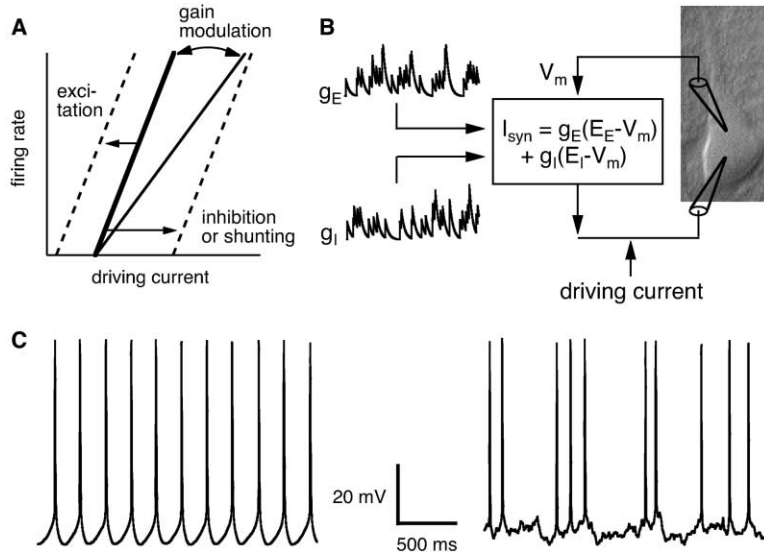
[3]Correspondence: chance@cns.nyu.edu

Figure 1. Simulating Background Synaptic Input with the Dynamic Clamp

(A) The thick solid trace represents a hypothetical plot of the firing rate of a neuron as a function of injected current. Adding excitation shifts the curve to the left, and inhibition (whether hyperpolarizing or shunting) shifts it to the right (dashed traces). Gain modulation, on the other hand, corresponds to a tipping of the firing-rate curve resulting in a change of its slope (thin solid trace).

(B) The dynamic clamp was used to simulate in vivo background synaptic conductances in vitro. Simulated excitatory and inhibitory synaptic conductances (g_E and g_I) were generated from independent Poisson spike trains. The synaptic current, I_{syn}, was computed by multiplying these computer-generated conductances by the difference between the measured membrane potential and the synaptic reversal potentials (equation in box). The computed synaptic current was then injected into the neuron along with an additional constant driving current.

(C) Membrane potential recorded from a neuron firing in response to a constant driving current without (left) and with (right) mimicked background synaptic input.

fluctuations, mimicking in vivo conditions, into neurons recorded in vitro. Neurons in a slice preparation receive little synaptic input because of the general lack of spontaneous activity in the slice. To study the effects of background input in a slice preparation, we used a computer-controlled dynamic clamp (see Experimental Procedures) to mimic, in single in vitro neurons, the conductance changes caused in vivo by the firing of populations of excitatory and inhibitory presynaptic neurons (Figure 1B) (see also Destexhe et al., 2001). In brief, the computer simulated the firing of excitatory and inhibitory afferent populations using independent random Poisson processes. With each excitatory or inhibitory presynaptic action potential, a unitary conductance, equivalent to that mediated by either AMPA or GABA$_A$ receptors (see, for example, Destexhe and Paré, 1999), was added to running tallies of total excitatory or inhibitory synaptic conductance, respectively. These conductances were then introduced into the cell under dynamic clamp via two electrodes patched on the soma.

To simulate typical in vivo conditions, excitatory inputs were generated at a rate of 7000 Hz and inhibitory inputs at a rate of 3000 Hz, representing the summed effects of many simulated afferents. We refer to this as the 1X condition. For the synaptic conductances and reversal potentials we used, these rates imply that the average total synaptic current reverses at −57 mV, and that excitatory and inhibitory contributions to the total synaptic current approximately cancel each other at typical membrane potentials. Because the excitatory and inhibitory synaptic inputs that make up the background synaptic activity were in such a balanced configuration, high levels of input noise and shunting could be introduced without producing excessive hyperpolarization or depolarization. We use the term input noise to mean specifically the variance of the total synaptic input current, and shunting to mean the change in total conduc-

tance due to the combined effects of excitatory and inhibitory synaptic inputs. The input rates and sizes of the unitary synaptic conductances were chosen so that the resulting barrage of background synaptic input affected the neuron in a manner consistent with in vivo measurements: shunting by background synaptic input increased the conductance of the neuron by two to three times its resting value (Bernander et al., 1991; Rapp et al., 1992; Borg-Graham et al., 1998; Hirsch et al., 1998; Destexhe and Paré, 1999), and the associated fluctuations in the total synaptic current (the input noise) induced fluctuations with an amplitude of a few millivolts in the membrane potential (Anderson et al., 2000a), changing the pattern of spiking in response to injected driving current from regular to irregular (Figure 1C).

The irregularity of spiking and general response variability introduced by the dynamic clamp input (see Figures 1C, 3E, and 3F) is toward the low end of the range measured in vivo. This level of variability is roughly the limit of what can be achieved with reasonable unitary synaptic conductances driven by uncorrelated inputs, which is what we used. More variable responses can be obtained by using correlated synaptic input (Stevens and Zador, 1998; Hô and Destexhe, 2000), but we decided against this both because of uncertainties about the amount and nature of the correlations that exist in vivo, and because the gain modulation effect we report is most robust when variability is high (discussed later; and see Figure 4). Thus, the conservative levels of variability produced by uncorrelated synaptic input provide a more rigorous test of the mechanism.

Multiplicative Gain Modulation of Neurons In Vitro

The point of our study is not only to introduce realistic background synaptic input into the quiet environment of the slice but also to see how varying its level affects neuronal responses. We modified the level of back-

ground synaptic input by scaling the computer-generated excitatory and inhibitory input rates by the same factor, which we call the rate factor (going to 2X or 3X conditions refers to doubling or tripling both input rates, for example). This manipulation increases both the input noise (the variance of the synaptic current) and the amount of shunting (the average total synaptic conductance) in proportion to the rate factor. Specifically, the average amount of shunting for excitatory and inhibitory inputs with rates r_E and r_I, peak unitary conductances g_E and g_I, synaptic decay constants τ_E and τ_I, and reversal potentials E_E and E_I is given by $g_E\tau_E r_E + g_I\tau_I r_I$, and the variance of the fluctuations in the total synaptic current at membrane potential V is proportional to $g_E^2\tau_E r_E(V - E_E)^2 + g_I^2\tau_I r_I(V - E_I)^2$. Because the background input is in a balanced configuration, equal scaling of excitatory and inhibitory input rates produces little net hyperpolarization or depolarization.

To characterize neuronal responses, we drove the neuron by injecting constant current, which we call driving current, along with the mimicked background synaptic input. We also performed studies in which neurons were driven by dynamic-clamp-generated excitatory synaptic inputs, rather than by injected current. Additional excitatory synaptic input introduces noise and shunting that are negligible in comparison to that produced by the balanced synaptic input. As a result, excitatory synaptic drive produces effects that are indistinguishable from those of constant injected current. For the experiments reported here, we used injected current to drive the neurons because this allows us to separate clearly the effects of excitatory drive from those of background synaptic input.

Figure 2A shows firing rates evoked by different amounts of driving current for various levels of background synaptic input (0X, closed diamonds; 1X, open circles; 2X, closed squares; 3X, open triangles). Increasing the level of background synaptic input made the neurons progressively less sensitive to changes in driving current, equivalent to modulating the gain of the neuronal response. The gains corresponding to the results in Figure 2A are plotted as a function of firing rate in Figure 2B (0X, closed diamond; 1X, open circle; 2X, closed square; 3X, open triangle). These gains were determined by taking the derivative of the best second-order polynomial fit to the firing-rate data. We plot the gain as a function of firing rate rather than driving current because this allows us to distinguish an additive (left-right) shift in a nonlinear firing-rate curve from a gain modulation. An additive shift in the firing-rate curve produces no change in a plot of gain versus firing rate, whereas a multiplicative modulation produces changes like those seen in Figure 2B.

We also determined average gains (rather than rate-dependent gains) by fitting straight lines to the nonzero portions of the firing-rate curves obtained using different levels of background input. The average gains, defined as the slopes of these straight-line fits, provide a single measure of response sensitivity. Figure 2C illustrates such linear fits and also shows gain modulation by background synaptic input in a different neuron than that shown in Figure 2A. The slopes of the fitted lines in Figure 2C are 34.4, 25.2, 17.5, and 12.7 Hz/nA in the 0X (closed diamonds), 1X (open circles), 2X (closed
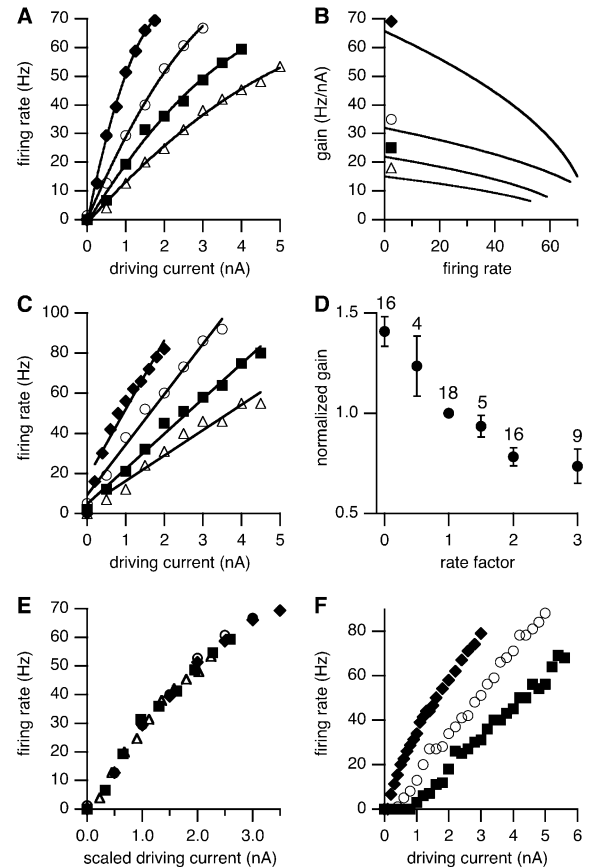

Figure 2. Changing the Level of Background Input Modulates Gain

(A) Firing rates of a representative neuron as a function of constant driving current without simulated background synaptic input (0X, closed diamonds), and with 1X (open circles), 2X (closed squares), and 3X (open triangles) background synaptic input. The solid lines are the best second-order polynomial fits to the data.

(B) The gains for the firing-rate curves in (A), defined as the derivatives of the polynomial fitting curves, plotted as a function of firing rate. Each trace is labeled by the symbol representing the corresponding case in (A).

(C) Firing rates of another neuron as a function of constant driving current under the same conditions as in (A) (0X, closed diamonds; 1X, open circles; 2X, closed squares; and 3X, open triangles). The solid lines are the best linear fits to the nonzero portions of the firing-rate curves.

(D) Average normalized gains for 18 different neurons as a function of the rate factor. Here, normalized gain is defined as the slope of the best linear fit to the nonzero portion of the firing-rate curve divided by the slope for a rate factor of one. Error bars are standard errors, and the numbers over each data point indicate the number of neurons tested in each condition.

(E) The firing-rate curves in (A) modified by appropriate scale factors to align them, with symbols as in (A). This indicates that gain modulation by background synaptic input is multiplicative. The 1X case appears unchanged from (A), but the driving currents for the 0X, 2X, and 3X data points were scaled by the factors 2, 0.65, and 0.45, respectively, while the firing rates were left unchanged.

(F) Example of a neuron for which the slope change in the firing-rate curve, due to changing the level of background synaptic input (0X, closed diamonds; 1X, open circles; and 2X, closed squares), is accompanied by a shift in the firing-rate curves.

squares), and 3X (open triangles) cases, respectively. Similar fits to Figure 2A yield 28.8, 22.5, 14.3, and 10.8 Hz/nA.

We studied gain modulation effects due to background synaptic input in 18 neurons, 15 of which showed consistent decreases in gain as the background input was increased across all levels tested. In Figure 2D, we characterize the gain of each neuron in each condition by the slope of the best straight-line fit to the corresponding firing-rate curve (as in Figure 2C) normalized by the gain of the neuron in the 1X condition. On average, changing the level of background input by rate factors ranging from 0 to 3 produced gain modulation by more than a factor of two, and this effect extended up to firing rates of at least 100 Hz. In these experiments, the same parameters were used for each neuron (see Experimental Procedures), which indicates that the mechanism of gain modulation does not require fine tuning.

Gain modulation by background synaptic input can be quite accurately multiplicative, as illustrated in Figure 2E, where the data points from Figure 2A have been scaled by appropriate factors to make them line up. This agrees with observations in a variety of in vivo systems where gain modulation is also multiplicative (Andersen and Mountcastle, 1983; Andersen et al., 1985; McAdams and Maunsell, 1999a; Treue and Martínez-Trujillo, 1999; Peña and Konishi, 2001). The firing-rate curves in Figure 2E were aligned by applying scaling factors to the driving currents, but similar results can be obtained by scaling the firing rates instead. This is because the firing-rate curves are approximately described by a power-law over the range we examine (Miller and Troyer, 2002; Hansel and Van Vreeswijk, 2002). Gain modulation can have different functional consequences depending on the nature of the scaling involved (Reynolds et al., 2000). We return to this issue in a later section.

For the fixed set of parameters we used in generating the background synaptic input, some of the neurons showed gain modulation that was not purely multiplicative because changing the rate factor shifted the firing-rate curves as well as changing their slopes. This shifting effect occurred at least in part because the parameters we used introduced a slight excess of inhibition. An example of such a shift, which is at the large end of the range for neurons showing significant gain modulation by background synaptic input, is shown in Figure 2F (0X, closed diamonds; 1X, open circles; 2X, closed squares). Purely multiplicative gain modulation could be obtained for this neuron by adjusting the balance between the inhibitory and excitatory components that make up the background synaptic input (see below), but we did not do this because we wanted to avoid fine tuning of parameters for each of the neurons studied.

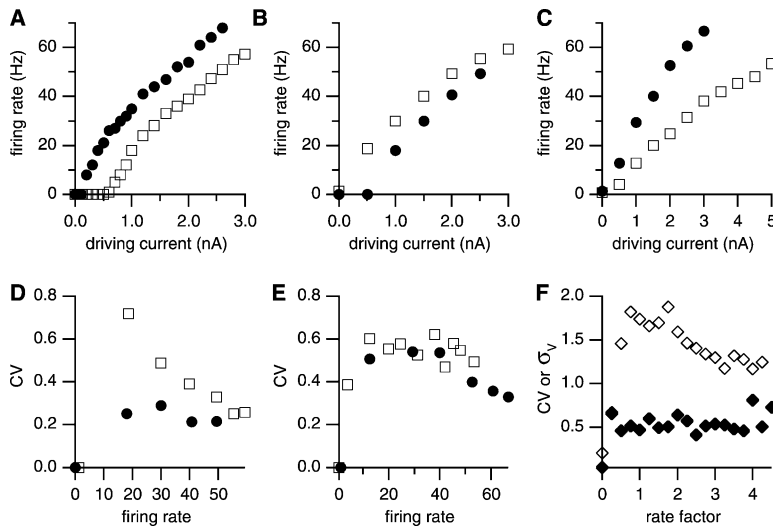**Contributions of Shunting and Noise
to Gain Modulation**
Increasing the rate of background synaptic input increases both the level of input noise and the amount of shunting. Because shunting produces a change in the input resistance (R), which affects the relationship between input current (I) and membrane potential (V) in a multiplicative manner ($V = IR$), it is often assumed that multiplicative gain modulation of neuronal responses can be generated purely by shunting. However, a theoretical study by Holt and Koch (1997) shows that this assumption is incorrect in a variety of neuron models.

Shunting generates a shift rather than a slope change in the firing-rate curve, similar to what occurs with hyperpolarizing inhibition (Figure 1A). For example, the firing rate of an integrate-and-fire model, for sufficiently high rates, is approximately proportional to $(A + IR)/\tau_m$, where A is a constant and τ_m is the effective membrane time constant (see, for example, Dayan and Abbott, 2001). This shows the expected dependence on the depolarization IR, but also includes a dependence on the membrane time constant τ_m, because this parameter sets the time scale for the dynamics of the model. Substituting the definition $\tau_m = RC$ into the above expression yields a firing rate proportional to $(A + IR)/RC = A/(RC) + I/C$. The first term in this expression produces an additive shift in the firing-rate curve when R is modified by shunting, but the second term, which determines the dependence of the firing rate on the input current, is independent of R and is thus unaffected by shunting. This explains why increased shunting shifts rather than tips firing-rate curves; decreasing R leads to less depolarization (IR), but this effect is cancelled by a decrease in the membrane time constant (RC).

To determine whether the theoretical arguments given above and in Holt and Koch (1997) apply to the neurons we studied, we used the dynamic clamp to introduce a shunting conductance equivalent to that introduced by the 2X background synaptic input (32 nS) used in Figures 1 and 2, but without any accompanying input noise. The reversal potential for this constant conductance was set equal to the conductance-weighted average of the excitatory and inhibitory reversal potentials of the background synaptic input (−57 mV). In agreement with the theoretical results, we found that increased shunting shifted the firing-rate curve but did not change its slope (n = 8; for an example see Figure 3A, control [closed circles], with additional conductance [open squares]).

Increasing the rate of background synaptic input increases the input noise as well as the amount of shunting. Because shunting alone does not change the slope of the firing-rate curve, we next consider the role that input noise plays in the gain modulation effect. To examine the effects of noise alone, we used the dynamic clamp to change the level of input noise without modifying the amount of synaptic shunting. This is done by multiplying the unitary synaptic conductances and dividing the input firing rates by the same factor (whereas changing the level of background input corresponds to scaling firing rates without changing unitary synaptic conductances). The average synaptic conductance remains constant with this manipulation because it is proportional to the product of the unitary synaptic conductance and the input firing rate. On the other hand, the input current variance increases because it is proportional to the square of the unitary synaptic conductance times the input rate.

Figure 3B shows the effects of using the dynamic clamp to increase input noise without changing the mean levels of total excitatory or inhibitory conductance (control, closed circles; with additional noise, open squares). It is well known that input noise enhances neuronal responses (see, for example, Hô and Destexhe, 2000), as seen in this figure. However, an important and less appreciated feature shown in Figure 3B is that the enhancement is not uniform across different levels of

Figure 3. Separate Effects of Shunting and Noise on Response Gain and Variability

(A) Firing rate versus constant driving current for a neuron without (closed circles), and with (open squares) 32 nS of additional constant conductance in the absence of any additional noise from background synaptic input. The result is a pure shift of the firing-rate curve.

(B) Firing rate versus constant driving current for a different neuron in the 1X condition (closed circles) and with the same level of conductance but input noise equivalent to the 3X condition (open squares). The effect is an increase in firing rate that is largest at low rates, resulting in a change in the slope of the firing-rate curve.

(C) The firing-rate curves for the 1X (closed circles) and 3X (open squares) conditions replotted from Figure 2A for comparison with (A) and (B).

(D) The coefficient of variation (CV) of the interspike intervals for the low (closed circles) and high (open squares) noise conditions shown in (B), plotted against firing rate. Increasing the level of input noise increases the CV.

(E) The CV of the interspike intervals for the 1X (closed circles) and 3X (open squares) conditions shown in (C), plotted against firing rate. Increasing the level of background synaptic input has little effect on the CV.

(F) Standard deviation of the membrane potential (open diamonds) in the absence of any driving current, for which the neuron in (C) did not fire, and the CV of the interspike intervals (closed diamonds) when the same neuron was driven to fire at approximately 20 Hz, plotted as a function of the rate factor. Both measures of response variability are roughly constant and independent of the rate factor, other than when it is zero.

driving current or, equivalently, firing rates. The rate-enhancing effect of input noise is most pronounced at low firing rates, and it decreases steadily as the firing rate increases. This induces a slope change in the firing-rate curve (Figure 3B; n = 6). In other words, increasing input noise *increases* the magnitude of the neuronal response for a given level of driving current, but it *decreases* the sensitivity of the response to changes in this current. Only the first of these effects has been widely discussed (although see Doiron et al., 2001).

Although a complete analysis of the effects of noise on neuronal firing is complex (see, for example, Ricciardi, 1977) we can provide an intuitive explanation for why noise enhances firing rates and why this effect diminishes at high rates. In the absence of noise and at a low firing rate, the membrane potential spends an appreciable amount of time hovering slightly below the threshold for action potential generation before the neuron fires. Noise-induced fluctuations can cause the neuron to fire earlier than it would have fired in the absence of noise at any time during this hovering period. This effect causes the increase in firing rate at low rates. However, when the neuron is firing rapidly, the membrane potential rises quickly to threshold without a significant hovering period. In this situation, balanced excitation and inhibition have roughly equal and opposite average effects on spike timing. Thus, at high firing rates, noise produces little net enhancement of firing rate.

Gain modulation by background synaptic input, as seen in Figure 3C, is the combined result of a noise-induced slope change (Figure 3B) and a shunting-induced rightward shift (Figure 3A). A consequence of these combined effects is that, unlike what happens with noise alone (Figure 3B), increasing the level of background input decreases response gain without the accompanying overall enhancement of firing (Figure 3C,

1X, closed circles; 3X, open squares). In other words, increasing balanced synaptic input *decreases* the sensitivity of the response to changes in driving current while *decreasing* the magnitude of the neuronal response for a given level of driving current. In summary, an increase in input noise causes a leftward shift and a slope change in the firing-rate curve, and shunting causes a rightward shift. A balanced increase in background synaptic input causes both to occur, and the left and right shift cancel, leaving a pure gain decrease.

Effects of Background Input
on Response Variability

Although varying the amount of input noise is crucial for changes in gain, gain modulation by this mechanism is not accompanied by significant changes in the response variability of a neuron. We quantified the degree of response variability by measuring the coefficient of variation (CV) of the interspike intervals and the variance of the subthreshold membrane fluctuations for the recorded neurons. Although increasing the amount of input noise with a fixed level of shunting (as in Figure 3B) increases response variability (Figure 3D, control, closed circles; additional noise, open squares), changing the level of background synaptic input (as in Figure 3C) does not (Figure 3E, 1X, closed circles; 3X, open squares; and Figure 3F). When background input rates were quadrupled from the 1X condition, the CV did not change appreciably (Figures 3E and 3F, closed diamonds), and the standard deviation of subthreshold membrane potential fluctuations changed by less than 30% (Figure 3F, open diamonds; these were measured at a level of driving current that produced no action potentials). Thus, background synaptic input acts as a source, but not as a modulator, of response variability.

Instead, as we have shown, it acts as a modulator of response gain.

Response variability does not vary appreciably with the level of background synaptic input over the range we consider because the effects of the increased input noise are cancelled by increased synaptic shunting. We can illustrate this directly in a passive neuron model (without spiking) for the case of subthreshold membrane potential fluctuations (also see Figure 3F for experimental data). The synaptic current arising from incoming Poisson spike trains that activate conductances with an instantaneous rise time and a decay time constant τ_s has a correlation function that decays exponentially with time constant τ_s, and which has an amplitude equal to σ_I^2, the variance of the synaptic current. In a passive neuron model, the membrane potential is simply a low-pass filtered version of the synaptic current, and the relationship between the current and voltage fluctuations can be computed in a straightforward manner to give $\sigma_V^2 = \sigma_I^2 \tau_s / (g^2(\tau_m + \tau_s))$ for the variance of the voltage fluctuations, where g is the total conductance (the sum of the intrinsic membrane conductance and the average synaptic conductance) and τ_m is the effective membrane time constant. For the parameters we use, the total conductance of the neuron is dominated by synaptic contributions (typically the background synaptic conductance is two or more times bigger than the membrane conductance) and $\tau_m > \tau_s$. Under these conditions, when balanced synaptic input rates are scaled by a rate factor x, $\sigma_I^2 \rightarrow x\sigma_I^2$, $g \rightarrow xg$, and $\tau_m \rightarrow \tau_m/x$ to a good approximation. This makes the variance of the fluctuations in the membrane potential approximately independent of the rate factor, because $\sigma_V^2 \approx \sigma_I^2 \tau_s / (g^2 \tau_m) \rightarrow x\sigma_I^2 \tau_s / (x^2 g^2 \tau_m / x) = \sigma_V^2$. Increasing background synaptic input rates increases both the variance of the input current and the overall conductance in such a way that there is no significant increase in the variance of membrane potential fluctuations. This translates into approximately constant spike-train variability as well.

Gain Modulation in a Model Neuron

Gain modulation through background synaptic input (Figure 3C) relies on a combination of the change in the slope of the firing-rate curve due to input noise (Figure 3B) and the rightward shift of the curve due to shunting (Figure 3A). A multiplicative effect, as in Figure 2E, will arise only if the rightward shift of the curve is of the appropriate magnitude (for example, Figure 4D shows what happens when the shift is too small). Furthermore, achieving gain modulation over an appreciable range of firing rates requires sufficiently high levels of input noise. To explore the sensitivity of gain modulation to these requirements, we used a modeling approach in which parameters can be varied freely.

We observed gain modulation through background synaptic input in a variety of models, ranging from relatively realistic conductance-based descriptions to simplified integrate-and-fire neurons. Here, we report results using a particularly convenient approach, an analytic expression for the firing rate of an integrate-and-fire neuron receiving noisy input (Ricciardi, 1977). To adapt this approach for our purposes, we approximate the background synaptic input by an equivalent
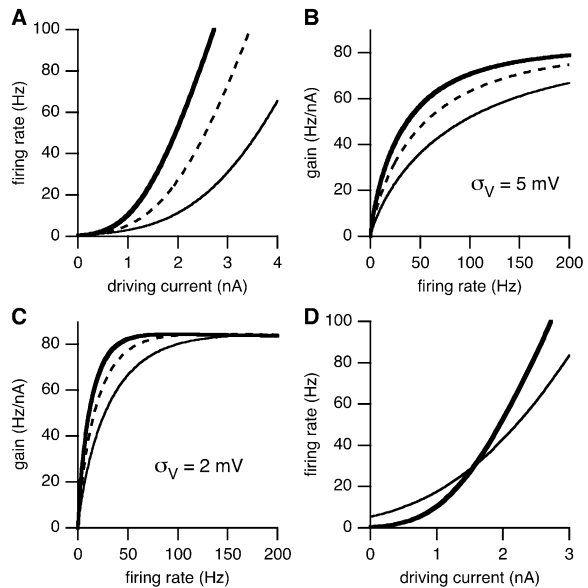

Figure 4. Gain Modulation in a Model Neuron

(A) Firing rate versus driving current from the analytic model for the 1X (thick trace), 2X (dashed trace), and 4X (thin trace) conditions. The standard deviation of the membrane potential fluctuations was 5 mV.

(B) Gain versus firing-rate curves for 1X (thick trace), 2X (dashed trace), and 4X (thin trace) conditions as in (A).

(C) Same as (B) but for membrane potential fluctuations of 2 mV.

(D) The thick trace is the firing rate versus driving current in the 1X condition described in (A). For the thin trace, the excitatory input rates were scaled by 5.3 and the inhibitory rates by 4.

white-noise current source and an equivalent shunting conductance (see Appendix). The resulting expression for the firing rate depends on the driving current I, the total conductance of the neuron g, and the variance of the membrane potential fluctuations produced by the white noise, σ_V^2. Because σ_V^2 is approximately independent of the level of background input, as seen in Figure 3F and discussed above, we simplify the analysis by treating it as a constant.

The analytic model displays gain modulation analogous to that shown in Figures 2A and 2B for the recorded neurons (Figures 4A and 4B, 1X, thick trace; 2X, dashed trace; 4X, thin trace). Although the shapes of the firing rate and gain curves are different for the model and real neurons, noise affects the real and model neurons in qualitatively similar ways. We found that the real neurons were more sensitive to noise than the model neurons we studied, and therefore gain modulation effects could be obtained in the real neurons using lower levels of input noise than in the model.

The rate-dependent enhancement of firing due to input noise (Figure 3B) fades at high firing rates. Because gain modulation relies on this effect, the gain changes are restricted to firing rates below some critical value. For the mechanism to be a viable candidate for the types of gain modulation seen in vivo, this critical rate must be sufficiently high. Figure 4B shows the gain modulation produced by changing background input rates when the noise-induced membrane potential fluctuations have a standard deviation of 5 mV. In this condition, the model

reveals significant gain modulation over the entire range of firing rates from 0 to 200 Hz. However, when the membrane potential fluctuations have a standard deviation of only 2 mV, gain modulation diminishes above about 50 Hz (Figure 4C, 1X, thick trace; 2X, dashed trace; 4X, thin trace). This indicates that noise levels of approximately 5 mV are needed to make the mechanism viable. We suggest that the large membrane potential fluctuations measured in vivo (see, for example, Anderson et al., 2000a) may be present to support gain modulation through background synaptic input over a wide range of firing rates.

Doiron et al. (2001) have noted previously, in a modeling study of voltage-dependent inhibition in neurons of the electrosensory lateral line lobe, that the combined effects of shunting and noise can have a multiplicative effect on firing rates. However, the effect they reported was limited to low firing rates because it involved noise arising solely from inhibitory input. This produces considerably smaller voltage fluctuations than the balanced combination of excitation and inhibition that we study.

For gain modulation to be multiplicative, as in Figure 2E, the amount of shunting and the amount of noise introduced by the background synaptic input must be appropriately matched. This might be a source of concern because, in our experiments, the dynamic clamp simulates synaptic conductances located at or near the soma of the neuron. Distal synapses can contribute to the input noise, but they may not produce much shunting. In the balanced configuration we use, shunting arises primarily from inhibitory inputs, and the noise is dominated by excitation. Thus, our results should apply even if the excitatory inputs are too distal to produce shunting, provided that inhibitory synapses are proximal enough to do so.

However, another effect can compensate if the shunting-induced shift of the firing-rate curve is too small (or, for that matter, if it is too large). Recall from Figure 1A, that ordinary excitation and inhibition also shift the firing-rate curve. Therefore, any deficiencies in the amount of shifting produced by shunting can be compensated for by adjusting the ratio of excitation to inhibition that make up the background synaptic input. For example, introducing a slight excess of inhibition over excitation within the mixture of background synaptic input can compensate for the fact that distal inputs might produce insufficient shunting to completely shift the firing-rate curve to its appropriate position, as we have verified in modeling studies.

Nevertheless, multiplicative gain modulation requires an appropriate combination of the effects of shunting and the degree of balance between excitation and inhibition. Figure 4D shows what happens if this condition is not met. In this example, the excitatory rate was increased 1.3 times as much as the inhibitory rate when background input was increased (rather than in a one-to-one ratio as for all the other figures). This has no effect on the noise-induced slope change of the firing-rate curve, but it causes the rightward shift seen in the transition from Figure 3B to 3C to be incomplete, so that the firing-rate curves cross. Thus, instead of the firing-rate curves for different gains converging at zero, they converge at approximately 35 Hz in this example.

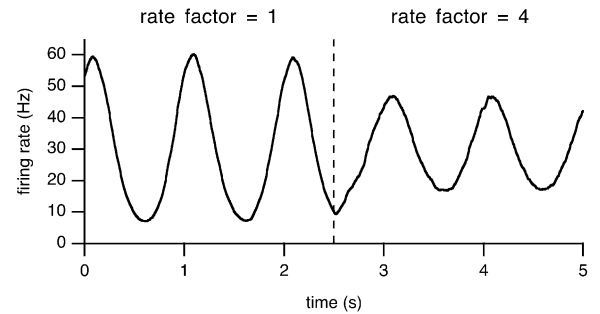Although the curves in Figure 4D no longer look like

Figure 5. Modulating the Gain of the Response to an Oscillatory Input

The firing rate of an integrate-and-fire model neuron driven by sinusoidally oscillating (1 Hz) current. For times less than 2.5 s, the neuron was in the 1X condition (thick trace in Figure 4D). At 2.5 s, the background input to the neuron was increased as it was for the thin trace in Figure 4D, but the oscillating input remained the same. The resulting gain modulation reduced the amplitude, but not the average level, of the response.

the gain-modulated curves in Figure 4A, they still display a form of response scaling that can be a useful feature, as illustrated in Figure 5. In this example, an oscillating driving current caused oscillations in the firing rate of an integrate-and-fire neuron. When the level of background synaptic input was modified at 2.5 s during the middle of the trace in Figure 5, the amplitude of the response oscillations, but not the average level of the response, decreased. This result, which is quite distinct from what could be obtained by conventional inhibitory effects, arises because the crossing point for the firing-rate curves was equal to the average response rate.

While the effect shown in Figure 5 is fairly modest, significantly larger effects can be obtained when neurons are connected together in a network. Recurrent excitation in such a circuit can amplify neuronal responses. In this case, reducing the gain of the neurons has two effects: it reduces their responsiveness to external input; and it also decreases the impact of the excitatory drive that they exert on each other. Because of this dual effect, the impact of gain modulation on the responses of network neurons can be considerably larger than what is seen for the single neuron in Figure 5, as we have verified in model networks (results not shown).

We can use the analytic model to investigate one more issue related to gain modulation, the nature of the multiplicative scaling produced by background synaptic input (Figure 2E). Examination of the analytic expression for the firing rate indicates that the relevant scaling factor in the model is $g\sigma_V$ (see Appendix). Over the range we study, this factor varies in proportion to the rate factor x. In the Appendix, we show that, under appropriate conditions, the dependence of the firing rate on the rate factor x and the driving current I is of the form $xF(I/x)$, where F is a nonlinear function. Thus, multiplicative gain modulation of the firing rate in the analytic model arises from a combination of divisive scaling of the current and multiplicative scaling of the firing rate. Although gain modulation in more realistic models and in real cells may exhibit more complex scaling laws, this

example provides a tractable case illustrating the basic features of the effect.

Discussion

Predictions

The mechanism we propose predicts that gain modulating signals, whether proprioceptive (Andersen and Mountcastle, 1983; Andersen et al., 1985), attentional (McAdams and Maunsell, 1999a; Treue and Martínez-Trujillo, 1999), or from other sources (Heeger, 1992; Peña and Konishi, 2001), are carried by a combination of excitatory and inhibitory inputs with firing rates that rise and fall together. Gain modulation by background synaptic input has two critical signature features. First, increases in gain are associated with decreases in background synaptic input and neuronal conductance. Second, the change in conductance during gain modulation is not accompanied by a significant modification in the variance of the membrane potential fluctuations or the variability of the spiking response. This last prediction agrees with data showing that spike-train variability was not affected by shifts in attention that multiplicatively scaled the amplitude of neural responses (McAdams and Maunsell, 1999b).

The background input that controls gain may arise from many sources: local circuits, distal sources, or feedback pathways (Bastian, 1986; Koch and Ullman, 1985; Hupé et al., 1998; Przybyszewski et al., 2000). If local excitatory and inhibitory synaptic connections provide significant, balanced synaptic input, a strong population response evoked by a potent stimulus (such as a high-contrast image in the case of the visual system) will generate a high level of balanced synaptic input that will lower response gain. This can produce the type of divisive response normalization that has been proposed to account for a number of observed phenomena in primary visual cortex, including response saturation (Heeger, 1992).

Background input from distal sources could be responsible for effects associated with attention, by increasing gain for attended stimuli. Interactions between locally and distally generated background inputs could explain why little attentional gain modulation is seen for high-contrast visual images (Reynolds et al., 2000). According to the proposed mechanism, attentional enhancement requires a reduction in the background input from sources controlling attention. However, for high-contrast images, the large amount of locally generated background input responsible for response saturation could mask the attention-related reductions in background input coming from distal sources.

Finally, gain modulation could be generated by background synaptic input arising from feedback pathways. Although such pathways are excitatory and tend to terminate on distal dendrites, they could generate balancing inhibition and the accompanying conductance changes by exciting local interneurons. If so, strong responses in a secondary area, which is the source of the feedback signal, could reduce the gain of responses in a primary sensory area. Conversely, neurons in the primary area would remain at high gain if they failed to generate a strong response in the secondary area

controlling their gain. In addition to assuring that signals of different efficacy all get transmitted from the primary to the secondary area, such feedback can lead to pop-out effects in which responses to unexpected stimuli, such as visual patches that differ from a background pattern, are enhanced (Rao and Ballard, 1999).

Conclusion

Sherman and Guillery (1998) have proposed that neurons have two classes of inputs, one responsible for driving neural responses and the other for modulating those responses. At the level of ionotropic synapses that could generate both fast responses and rapid modulation, it is not clear what anatomical basis exists for this dual classification. We suggest that the two classes of inputs are not defined anatomically, but rather, functionally. Sets of balanced inputs that have excitatory and inhibitory rates rising and falling together comprise modulatory inputs, and those for which excitation and inhibition vary in opposite directions act as driving inputs. This arrangement has the advantage that individual excitatory inputs can rapidly switch between driving and modulatory functions, depending on whether they are varying in parallel with or in opposition to changes in inhibition.

Neurons receiving large amounts of background excitatory and inhibitory input operate quite differently from the conventional picture of neuronal input integration. Our observation that levels of background input modify response gain suggests that such activity is not simply a source of response variability, but instead, plays an important role in controlling cortical processing. In summary, we propose that cortical neurons in vivo operate in a transistor-like mode in which sets of excitatory and inhibitory inputs with covarying firing rates act as gain control signals to gate other sets of driving inputs with opposing, push-pull excitation and inhibition.

Experimental Procedures

Slices of rat somatosensory cortex were prepared for whole-cell recording as described previously (Reyes and Sakmann, 1999). Rats were anesthetized with halothane and decapitated. One hemisphere of the brain was then removed, and 300 μm slices were cut in ice-cold artificial cerebrospinal fluid or ACSF (125 mM NaCl, 25 mM NaHCO$_3$, 25 mM glucose, 2.5 mM KCl, 1.25 mM NaH$_2$PO$_4$, 2 mM CaCl$_2$, 1 mM MgCl$_2$), using a vibratome tissue slicer. During recording, slices were perfused with 30°C ACSF bubbled with 95% O$_2$, 5% CO$_2$. Simultaneous whole-cell somatic recordings from layer 5 pyramidal neurons were performed under dynamic clamp using two electrodes, patched at the soma, filled with 100 mM K-gluconate, 20 mM KCl, 10 mM phosphocreatine, 10 mM HEPES, 4 mM ATP-Mg, and 0.3 mM GTP at pH 7.3 (filled electrode resistances ranged from 5 to 10 MΩ). The dynamic clamp is a voltage-controlled current clamp (Sharp et al., 1993; Robinson and Kawai, 1993) that uses an analog multiplier to calculate and inject the current that would be produced by computer-determined conductance changes. With the dynamic clamp, one electrode was used for current injection and the other to record the neuronal membrane potential. Recordings were terminated if neurons were spontaneously firing or had an initial resting potential above −55 mV, or if either electrode had an initial access resistance greater than 50 MΩ.

Excitatory and inhibitory synaptic currents were calculated using an analog multiplier as $I_{syn} = g_{syn}(E_{rev} - V)$, where g_{syn} is the computer-controlled synaptic conductance generated from simulated presynaptic spike trains, E_{rev} is the reversal potential of the synaptic con-

ductance (0 mV for excitatory inputs and −80 mV for inhibitory inputs), and *V* is the measured membrane potential of the neuron. Presynaptic spike trains were generated by Poisson processes at the specified rates. The unitary synaptic conductance for each presynaptic spike was calculated as a difference of exponentials, with time constants of 0.1 ms for the rising phase and either 5 ms (excitatory) or 10 ms (inhibitory) for the falling phase. The peak unitary synaptic conductances were set to 2% (excitatory) or 6% (inhibitory) of the measured resting membrane conductance. The same parameters were used for all the neurons studied.

A step of constant driving current lasting 2–3 s was injected along with the simulated background synaptic input. The firing rate was measured after 500 ms of stimulation by counting the number of action potentials over the remaining stimulus time interval and dividing by its duration. Trials were separated by a recovery period of at least 10 s.

The analytic formula used for Figure 4 describes the firing rate of an integrate-and-fire model with input consisting of white noise and constant current and is discussed in the Appendix. In addition to the parameters given in the text, the firing rate in the analytic model depends on the resting value of the membrane time constant (taken to be 20 ms) and the difference between the action potential threshold and reset membrane potentials (taken to be 6 mV following the analysis of Troyer and Miller [1997]). For the 1X condition, we assumed that the background synaptic input produced a synaptic conductance equal to the resting conductance of the neuron.

The integrate-and-fire model in Figure 5 had a resting membrane potential $V_{rest} = -65$ mV, an action potential threshold $V_{th} = -54$ mV, and a postspike reset potential $V_{reset} = -60$ mV. The synaptic dynamics was identical to that used for the real neurons, except that the rise of the synaptic conductances was taken to be instantaneous. The parameters describing the background synaptic input were adjusted to produce subthreshold membrane potential fluctuations with a standard deviation of 5 mV (total excitatory and inhibitory synaptic conductances equal to 0.4 and 1.6 times the resting membrane conductance, with rates of 135 Hz for both). The firing rate in response to an oscillating driving current was extracted by counting spikes and averaging over multiple runs.

Appendix

The analytic expression for the firing rate *r* of an integrate-and-fire neuron (with resting membrane conductance g_0, synaptic conductance g_s, resting membrane time constant τ_0, and action-potential threshold and reset voltages V_{th} and V_{reset}, receiving a constant current *I* and white noise current that produces membrane potential fluctuations with standard deviation σ_V, takes the form

$$r = \frac{g\sigma_v}{g_0(V_{th} - V_{reset})\tau_0} f\left(\frac{V_\infty - 0.5(V_{th} + V_{reset})}{\sigma_v}\right),$$

where $g = g_0 + g_s$ is the total membrane conductance and $V_\infty = (g_0V_0 + g_sV_B + I)/g$. V_0 is the resting potential of the neuron and V_B is the potential at which the excitatory and inhibitory synaptic currents sum to zero. An explicit expression for the function *f*, which is an integral of a combination of Gaussian and error functions, is not needed for our discussion (Ricciardi, 1977), and an additional dependence on the quantity $(V_{th} - V_{reset})/\sigma_V$ has been suppressed because this is a constant in the case we consider. To simplify the analysis, we take $V_0 = V_B = 0.5(V_{th} + V_{reset})$ from which it follows that $V_\infty = 0.5(V_{th} + V_{reset}) + I/g$ and

$$r = \frac{g\sigma_v}{g_0(V_{th} - V_{reset})\tau_0} f\left(\frac{I}{g\sigma_v}\right).$$

As discussed in the text, the combination $g\sigma_V$ varies approximately in proportion to the scale factor *x* when background input rates are varied. Thus, the above equation implies the relationship given in the text, $r \propto xF(I/x)$, with *F* closely related to *f*. The function *f* initially rises from zero with a nonlinear dependence on its argument, but for sufficiently large values of *I* it becomes linear. When this occurs, the factor of $g\sigma_V$ within *f* and the factor of $g\sigma_V$ multiplying *f* in the above equation cancel, and gain modulation goes away, as discussed in the text.

References

Andersen, R.A., and Mountcastle, V.B. (1983). The influence of the angle of gaze upon the excitability of light-sensitive neurons of the posterior parietal cortex. J. Neurosci. *3*, 532–548.

Andersen, R.A., Essick, G.K., and Siegel, R.M. (1985). Encoding of spatial location by posterior parietal neurons. Science *230*, 450–458.

Anderson, J.S., Lampl, I., Gillespie, D.C., and Ferster, D. (2000a). The contribution of noise to contrast invariance of orientation tuning in cat visual cortex. Science *290*, 1968–1972.

Anderson, J.S., Carandini, M., and Ferster, D. (2000b). Orientation tuning of input conductance, excitation, and inhibition in cat primary visual cortex. J. Neurophysiol. *84*, 909–926.

Bastian, J. (1986). Gain control in the electrosensory system mediated by descending inputs to the electrosensory lateral line lobe. J. Neurosci. *6*, 553–562.

Bernander, Ö., Douglas, R.J., Martin, K.A.C., and Koch, C. (1991). Synaptic background activity influences spatiotemporal integration in single pyramidal cells. Proc. Natl. Acad. Sci. USA *88*, 11569–11573.

Borg-Graham, L.J., Monier, C., and Frégnac, Y. (1998). Visual input evoles transient and strong shunting inhibition in visual cortical neurons. Nature *393*, 369–372.

Dayan, P., and Abbott, L.F. (2001). Theoretical Neuroscience (Cambridge, MA: MIT Press), p. 164.

Destexhe, A., and Paré, D. (1999). Impact of network activity on the integrative properties of neocortical pyramidal neurons *in vivo*. J. Neurophysiol. *81*, 1531–1547.

Destexhe, A., Rudolph, M., Fellous, J.-M., and Sejnowski, T.J. (2001). Fluctuating synaptic conductances recreate *in vivo*-like activity in neocortical neurons. Neuroscience *107*, 13–24.

Doiron, B., Longtin, A., Berman, N., and Maler, L. (2001). Subtractive and divisive inhibition: effect of voltage-dependent inhibitory conductances and noise. Neural Comput. *13*, 227–248.

Hahnloser, R.H., Sarpeshkar, R., Mahowald, M.A., Douglas, R.J., and Seung, H.S. (2000). Digital selection and analogue amplification coexist in a cortex-inspired silicon circuit. Nature *405*, 947–951.

Hansel, D., and Van Vreeswijk, C. (2002). How noise contributes to contrast invariance of orientation tuning in cat visual cortex. J. Neurosci. *22*, 5118–5128.

Heeger, D.J. (1992). Normalization of cell responses in cat striate cortex. Vis. Neurosci. *9*, 181–198.

Hirsch, J.A., Alonso, J.-M., Reid, R.C., and Martinez, L.M. (1998). Synaptic integration in striate cortical simple cells. J. Neurosci. *18*, 9517–9528.

Hô, N., and Destexhe, A. (2000). Synaptic background activity enhances the responsiveness of neocortical pyramidal neurons. J. Neurophysiol. *84*, 1488–1496.

Holt, G.R., and Koch, C. (1997). Shunting inhibition does not have a divisive effect on firing rates. Neural Comput. *9*, 1001–1013.

Holt, G.R., Softky, W.R., Koch, C., and Douglas, R.J. (1996). Comparison of discharge variability *in vitro* and *in vivo* in cat visual cortex neurons. J. Neurophysiol. *75*, 1806–1814.

Hupé, J.M., James, A.C., Payne, B.R., Lomber, S.G., Girard, P., and Bullier, J. (1998). Cortical feedback improves discrimination between figure and background by V1, V2 and V3 neurons. Nature *394*, 784–787.

Koch, C., and Poggio, T. (1992). Multiplying with synapses and neurons. In Single Neuron Computation, T. McKeena, J. Davis, and S. Zornetzer, eds. (Orlando, FL: Academic Press), pp. 315–345.

Koch, C., and Ullman, S. (1985). Shifts in selective visual attention: towards the underlying neural circuitry. Hum. Neurobiol. *4*, 219–227.

McAdams, C.J., and Maunsell, J.H.R. (1999a). Effects of attention on orientation-tuning functions of single neurons in macaque cortical area V4. J. Neurosci. *19*, 431–441.

McAdams, C.J., and Maunsell, J.H.R. (1999b). Effects of attention on the reliability of individual neurons in monkey visual cortex. Neuron *23*, 765–773.

Mel, B.W. (1993). Synaptic integration in an excitable dendritic tree. J. Neurophysiol. *70*, 1086–1101.

Miller, K.D., and Troyer, T.W. (2002). Neural noise can explain expansive, power-law nonlinearities in neural response functions. J. Neurophysiol. *87*, 653–659.

Peña, J.L., and Konishi, M. (2001). Auditory spatial receptive fields created by multiplication. Science *292*, 249–252.

Pouget, A., and Sejnowski, T.J. (1997). Spatial transformations in the parietal cortex using basis functions. J. Cogn. Neurosci. *9*, 222–237.

Przybyszewski, A.W., Gaska, J.P., Foote, W., and Pollen, D.A. (2000). Striate cortex increases contrast gain of macaque LGN neurons. Vis. Neurosci. *17*, 485–494.

Rao, R.R., and Ballard, D.H. (1999). Predictive coding in the visual cortex: a functional interpretation of some extra-classical receptive-field effects. Nat. Neurosci. *2*, 79–87.

Rapp, M., Yarom, Y., and Segev, I. (1992). The impact of parallel fiber background activity on the cable properties of cerebellar Purkinje cells. Neural Comput. *4*, 518–532.

Reyes, A., and Sakmann, B. (1999). Developmental switch in the short-term modification of unitary EPSPs evoked in layer 2/3 and layer 5 pyramidal neurons of rat neocortex. J. Neurosci. *19*, 3827–3835.

Reynolds, J.H., Pasternak, T., and Desimone, R. (2000). Attention increases sensitivity of V4 neurons. Neuron *26*, 703–714.

Ricciardi, L.M. (1977). Diffusion Processes and Related Topics in Biology (Berlin: Springer-Verlag).

Robinson, H.P.C., and Kawai, N. (1993). Injection of digitally synthesized synaptic conductance transients to measure the integrative properties of neurons. J. Neurosci. Methods *49*, 157–165.

Salinas, E., and Abbott, L.F. (1995). Transfer of coded information from sensory to motor networks. J. Neurosci. *15*, 6461–6474.

Salinas, E., and Abbott, L.F. (1996). A model of multiplicative neural responses in parietal cortex. Proc. Natl. Acad. Sci. USA *93*, 11956–11961.

Salinas, E., and Abbott, L.F. (1997) Invariant visual responses from attentional gain fields. (1997). J. Neurophysiol. *77*, 3267–3272.

Salinas, E., and Thier, P. (2000). Gain modulation: a major computation principle of the central nervous system. Neuron *27*, 15–21.

Shadlen, M.N., and Newsome, W.T. (1994). Noise, neural codes and cortical organization. Curr. Opin. Neurobiol. *4*, 569–579.

Sharp, A., O'Neil, M.B., Abbott, L.F., and Marder, E. (1993). The dynamic clamp: artificial conductances in biological neurons. Trends Neurosci. *16*, 389–394.

Sherman, S.M., and Guillery, R.W. (1998). On the actions that one nerve cell can have on another: distinguishing "drivers" from "modulators". Proc. Natl. Acad. Sci. USA *95*, 7121–7126.

Smith, M.R., Nelson, A.B., and du Lac, S. (2002). Regulation of firing response gain by calcium-dependent mechanisms in vestibular nucleus neurons. J. Neurophysiol. *87*, 2031–2042.

Softky, W.R., and Koch, C. (1993). The highly irregular firing of cortical cells is inconsistent with temporal integration of random EPSPs. J. Neurosci. *13*, 334–350.

Srinivasan, M.V., and Bernard, G.D. (1976). A proposed mechanism for the multiplication of neural signals. Biol. Cybern. *21*, 227–236.

Stevens C.F., and Zador, A.M. (1998). Input synchrony and the irregular firing of cortical neurons. Nat. Neurosci. *3*, 210–217.

Tiesinga, P.H.E., José, J.V., and Sejnowski, T.J. (2001). Comparison of current-driven and conductance-driven neocortical model neurons with Hodgkin-Huxley voltage-gated channels. Phys. Rev. E. Stat. Phys. Plasmas Fluids Relat. Interdiscip. Topics *62*, 8413–8419.

Treue, S., and Martínez-Trujillo, J.C. (1999). Feature-based attention influences motion processing gain in macaque visual cortex. Nature *399*, 575–579.

Troyer, T.W., and Miller, K.D. (1997). Physiological gain leads to high ISI variability in a simple model of a cortical regular spiking cell. Neural Comput. *9*, 971–983.

Zipser, D., and Andersen, R.A. (1988). A back-propagation programmed network that simulates response properties of a subset of posterior parietal neurons. Nature *331*, 679–684.